3D PHASE-FIELD FOR PRESSURIZED FRACTURE PROPAGATION IN HETEROGENEOUS MEDIA

THOMAS WICK[*,**,†]**, SANGHYUN LEE**[†] **AND MARY F. WHEELER**[†]

* Johann Radon Institute for Computational and Applied Mathematics,
Austrian Academy of Sciences,
4040 Linz, Austria
e-mail: thomas.wick@ricam.oeaw.ac.at,
web page: http://people.ricam.oeaw.ac.at/t.wick/

** Fakultät für Mathematik,
Technische Universität München,
85748 Garching bei München, Germany

† The Institute for Computational Engineering and Sciences,
The University of Texas at Austin,
Austin, Texas 78712, USA
e-mail: shlee@ices.utexas.edu
web page: http://users.ices.utexas.edu/∼shlee/

Key words: Phase-field, variational approach to fracture, pressurized cracks, porous media

Abstract. This work presents recent progress in phase-field-based fracture modeling in heterogeneous porous media. Existing algorithms that have been developed in the last years are extended to tackle three-dimensional configurations. Our solution technique is formulated in terms of a nested Newton loop that combines a primal-dual active set method (required for treating the crack irreversibility) and a Newton method to solve the nonlinear, fully-coupled PDE system. An advanced numerical test demonstrates the capabilities of our method.

1 INTRODUCTION

Crack propagation in elastic and porous media is currently one of the major research topics in mechanical, energy, and environmental engineering. In this paper, we concentrate specifically on pressurized-fracture propagation in heterogeneous media towards applications in porous media. Our method of choice is a variational approach for brittle fracture [9] that is formulated in terms of a phase-field technique. The methodology seems very promising as attested by several major publications in recent years [6, 7, 15, 14, 4, 2, 8].

Here, discontinuities in the displacement field across the lower-dimensional crack surface are approximated by an auxiliary phase-field function. This is an indicator function, which introduces a diffusive transition zone (brittle or mushy-zone are also common expressions depending on the discipline) between the broken and the unbroken material. Most importantly, fracture nucleation, propagation, kinking, and curvilinear paths are automatically included in the model; post-processing of stress intensity factors and remeshing resolving the crack path are avoided. Recent progress towards hydraulic fracturing scenarios has been made in [10] (using XFEM/GFEM), [13] (using peridynamics) [5, 1] (using variational fracture methods), and [18, 19] (phase-field methods that are related to variational techniques).

The crucial numerical aspects of a phase-field-based fracture propagation approach are techniques that include resolution of the length-scale parameter ε, the numerical solution of the forward problem and enforcement of the irreversibility of crack growth. The sum of these requirements leads to a variational inequality discretized in terms of an adaptive finite element scheme. A robust numerical framework has been proposed in [11] in which a primal-dual active set method [12] is combined with a Newton method for the forward problem and leading to a nested Newton loop.

The forward problem; namely, the coupled Euler-Lagrange PDE system is addressed monolithically in which both equations, elasticity and phase-field, are solved simultaneously. We propose a robust numerical scheme in terms of a Newton linearization to treat the non-convexity of the regularized energy functional and the consequences of non-convexity on the Euler-Lagrange system.

The **key aspect of this paper** is to extend these algorithms to three-dimensional applications and to demonstrate the potential of our method for two initially non-aligned cracks in a heterogeneous medium and their propagation leading two interaction through joining and branching. To the best of our knowledge such a result is novel for pressurized cracks computed with phase-field.

The outline of this work is as follows: We first state the governing equations in Section 2. Then, we briefly state our main algorithm in Section 3. A sophisticated 3D numerical example is presented in Section 4 in order to exploit the potential of our approach.

2   NOTATION AND EQUATIONS

In this section, we explain the governing equations. Here, we adopt an phase-field-based approach in terms of the Euler-Lagrange weak formulation for pressurized fractures that has been derived in [17, 18, 19]. The unknown solution variables are vector-valued displacements $\mathbf{u}$ and a smoothed indicator phase-field function φ with values in $[0, 1]$. For $\varphi = 0$, we denote a crack region and $\varphi = 1$ is the unbroken material. The intermediate values constitute a so-called transition zone that is dependent on a regularization (or length-scale) parameter ε. In particular, ε is the thickness of the transition zone. Due to the crack irreversibility condition,

$$\partial_t \varphi \leq 0,$$

the resulting system is a variational inequality.

Let $V := H_0^1(\Omega)$ and $W_{in} := \{w \in H^1(\Omega) | w \leq \varphi^{n-1} \leq 1 \text{ a.e. on } \Omega\}$ be the function spaces we work with; and for later purposes we also need $W := H^1(\Omega)$.

Formulation 1 (Variational inequality system for pressurized fractures) *Find* $(\mathbf{u}, \varphi) \in V \times W$ *with*

$$\Big(\big((1 - \kappa)\varphi^2 + \kappa\big)\, \sigma(\mathbf{u}), e(\mathbf{w})\Big) - (\alpha - 1)(\varphi^2 p,\, div\, \mathbf{w}) = 0 \quad \forall \mathbf{w} \in V, \tag{1}$$

as well as

$$\begin{aligned}
&(1 - \kappa)(\varphi\, \sigma(\mathbf{u}) : e(\mathbf{u}), \psi - \varphi) - 2(\alpha - 1)(\varphi\, p\, div\, \mathbf{u}, \psi - \varphi) \\
&+ G_c\Big(-\frac{1}{\varepsilon}(1 - \varphi, \psi - \varphi) + \varepsilon(\nabla\varphi, \nabla\psi - \varphi)\Big) \geq 0 \quad \forall\, \psi \in W_{in} \cap L^\infty(\Omega).
\end{aligned} \tag{2}$$

where, $\sigma = \sigma(\mathbf{u})$ *is the stress tensor,*

$$\sigma := \sigma(\mathbf{u}) = 2\mu e(\mathbf{u}) + \lambda\, tr(e(\mathbf{u}))I,$$

and $e(\mathbf{u})$ *the symmetric strain tensor defined as*

$$e(\mathbf{u}) := \frac{1}{2}\left(\nabla\mathbf{u} + \nabla\mathbf{u}^T\right).$$

and μ *and* λ *are material parameters,* I *is the identity matrix,* G_c *is the energy release rate* $G_c > 0$, ε *is the previously mentioned crack surface regularization parameter, and finally* κ *is a positive regularization parameter for the elastic energy, with* $\kappa \ll \varepsilon$.

This system is based on a quasi-stationarity assumption in which the time t *(i.e. in a quasi-stationary setting* t *is more a load parameter rather than true 'time') enters through time-dependent boundary conditions, e.g.,* $\mathbf{u} = \mathbf{u}(t) = \mathbf{g}(t)$ *on* $\partial\Omega_D$ *with a prescribed boundary function* $g(t)$ *of Dirichlet-type or through time-dependent right hand side forces, e.g.,* $p := p(t)$ *as used in our numerical example.*

Remark 2.1 *In poroelastic applications, the pressure* p *is obtained from solving a pressure Darcy equation. This coupled system is solved with a fixed-stress iteration [21, 16] in which the pressure equation and elasticity equation are solved sequentially. Correct modeling of interface forces [17, 19]* $\varphi^2\nabla p$ *where the fluid pressure in the crack interacts with poroelastic fluid flow. However, for a given, piece-wise constant, pressure this term is zero and neglected in the rest of this paper. In addition, Biot's coefficient is chosen as* $\alpha = 0$. *Both terms appear in situations as investigated in [20, 22, 23].*

3 NUMERICAL APPROXIMATION

Our solution algorithm is based on a combined Newton iteration (to compute an update δU_k^h such that $U_{k+1}^h = U_k^h + \delta U_k^h$, where k is the Newton iteration number, and h the spatial discretization parameter) that assembles the crack irreversibility with the help of a semi-smooth Newton method and a second Newton iteration for the fully-coupled forward problem. The problem is quasi-static and temporal derivatives are approximated with a backward difference scheme. Spatial discretization is based on Galerkin finite elements using trilinear ansatz and test functions.

In the following, let the (discrete) residual be denoted by $R(U_k^h) = -A(U_k^h)(\Psi^h)$ with $U_k^h := \{\mathbf{u}_k^h, \varphi_k^h\} \in V^h \times W^h$ and (now neglecting the indices k and h):

$$
\begin{aligned}
A(U)(\Psi) = &\Big(\big((1-\kappa)\tilde{\varphi}^2 + \kappa \big)\, \sigma(\mathbf{u}), e(\mathbf{w}) \Big) - (\alpha-1)(\tilde{\varphi}^2 p, \operatorname{div} \mathbf{w}) \\
& + (1-\kappa)(\varphi\, \sigma(\mathbf{u}) : e(\mathbf{u}), \psi) - 2(\alpha-1)(\varphi\, p \operatorname{div} \mathbf{u}, \psi) \\
& + G_c\Big(-\frac{1}{\varepsilon}(1-\varphi, \psi) + \varepsilon(\nabla\varphi, \nabla\psi) \Big) = 0 \quad \forall \Psi := \{\mathbf{w}, \psi\} \in V \times W.
\end{aligned}
\tag{3}
$$

In this system, the well-known difficulty; namely the non-convexity of the first term on the energy level, $\Big(\big((1-\kappa)\varphi^2 + \kappa \big)\, \sigma(\mathbf{u}), e(\mathbf{w}) \Big)$ is treated by replacing (the solution variable) φ by a (known) extrapolation $\tilde{\varphi}$ computed from two previous time steps. This heuristic procedure is very robust and yields excellent approximation properties with regard to the true φ. Verification in terms of benchmarks is provided in [11].

The corresponding Newton matrix is built by computing the directional derivative $A'(U_k^h)(\delta U_k^h, \Psi^h)$. Then, $\delta U_k^h := \{\delta \mathbf{u}_k^h, \delta\varphi_k^h\} \in V^h \times W^h$ such that

$$
\begin{aligned}
A'(U)(\delta U, \Psi) = &\Big(\big((1-\kappa)\tilde{\varphi}^2 + \kappa \big)\, \sigma(\delta\mathbf{u}), e(\mathbf{w}) \Big) \\
& + (1-\kappa)(\delta\varphi\sigma^+(\mathbf{u}) : e(\mathbf{u}) + 2\varphi\, \sigma(\delta\mathbf{u}) : e(\mathbf{u}), \psi) \\
& - 2(\alpha-1)p(\delta\varphi\operatorname{div} \mathbf{u} + \varphi \operatorname{div} \delta\mathbf{u}, \psi) \\
& + G_c\Big(\frac{1}{\varepsilon}(\delta\varphi, \psi) + \varepsilon(\nabla\delta\varphi, \nabla\psi) \Big) = 0 \quad \forall \Psi := \{\mathbf{w}, \psi\} \in V \times W.
\end{aligned}
\tag{4}
$$

Furthermore, $(B)_{ii}$ is a diagonal mass matrix [12].

The semi-smooth Newton method can be interpreted as a primal-dual active set method and vice versa [12]. With these preparations, we define our solution algorithm:

Algorithm 3.1 ([11]) *Repeat for $k = 0, 1, 2, \ldots$:*

1. *Assemble residual $R(U_k^h)$*

2. *Compute active set $\mathcal{A}_k = \{i \mid (B^{-1})_{ii}(R_k^h)_i + c(\delta U_k^h)_i > 0\}, \quad i : \text{ is a DoF}$*

3. *Assemble matrix $G = A'(U_k^h)(\cdot, \Psi^h)$ and right-hand side $F = -A(U_k^h)(\Psi^h)$*

4. *Eliminate rows and columns in* $\mathcal{A}_k$ *from* G *and* F *to obtain* $\widetilde{G}$ *and* $\widetilde{F}$

5. *Solve the linear system* $\widetilde{G}\delta U_k^h = \widetilde{F}$, *i.e,*

$$\widetilde{A}'(U_k^h)(\delta U_k^h, \Psi^h) = -\widetilde{A}(U_k^h)(\Psi^h) \quad \forall \Psi \in V^h \times W^h. \tag{5}$$

6. *Find a step size* $0 < \omega \leq 1$ *using line search to get*

$$U_{k+1}^h = U_k^h + \omega \delta U_k^h,$$

with $\widetilde{R}(U_{k+1}^h) < \widetilde{R}(U_k^h)$.

Finish if both stopping criteria are fulfilled simultaneously:

$$\mathcal{A}_{k+1} = \mathcal{A}_k \qquad and \qquad \widetilde{R}(U_k^h) < \text{TOL}.$$

4 NUMERICAL TEST: TWO PENNY-SHAPED FRACTURES IN A HETEROGENEOUS MEDIUM

In this final section, we present an advanced numerical example that demonstrates the capabilities for realistic scenarios of our method. This example is computed based on the finite element software deal.II [3] and based on an extension of the programming code developed for [11].
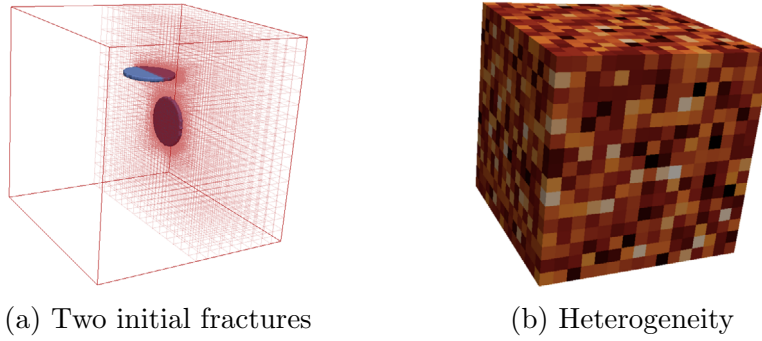

(a) Two initial fractures   (b) Heterogeneity

Figure 1: (a) Two initial penny shaped crack is position in the middle of the media. (b) Young's modulus(E) has the value range of the shale rock region; $E \in [1\,\text{GPa}, 10\,\text{GPa}]$ and $\nu = 0.15$.

We take a setting with two initial penny-shaped fractures in a 3D heterogeneous medium. The locally refined grid in the cube $\Omega = (0m, 4m)^3$ with hanging nodes is shown in Figure 1a. The cells around the crack interface are refined (if $\varphi(\mathbf{x}, t) < 0.8$) using the a predictor-corrector strategy [11]. In Figure 1a two initial fractures are described. The top fracture is centered at $(2, 3, 2)[m]$ with radius $r = 0.5m$ in $y = 3m$-plane and

the bottom fracture is centered at $(2.5, 2, 2)[m]$ with radius $r = 0.5m$ in $x = 2.5m$-plane. The crack is approximated as a volume by extending it with the spatial discretization parameter h. The thickness of both fractures are $2h_{\min}$. As outer boundary conditions we set the displacements zero on $\partial\Omega$.

The pressure is constant in space with $\alpha = 0$ in (1), but it is linearly increasing in time as $p = t \times 1\,\mathrm{MPa}[Pa]$, where t is the current time. The numerical constants are given as $k = 10^{-10} \times h_{\min}$ and $\varepsilon = 2h_{\min}$. Here $h_{\min} = 0.0541266m$ and the time steps are $dt = 0.01s$.

We observe joining and branching of non-planar fractures in heterogeneous media. Those are automatically captured by the phase field method. See Figure 2 and Figure 3 for the details. Finally, in Figure 3, the bulk and crack energies are observed. We clearly see that the crack energy remains constant while the cracks are not growing and this energy increases for growing fractures.
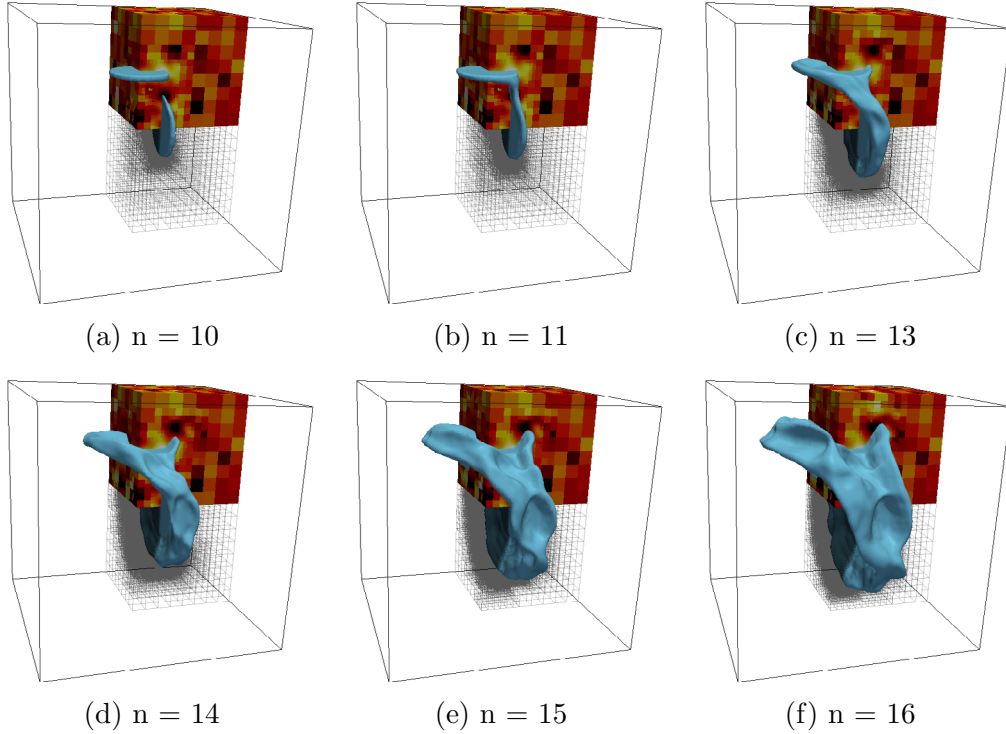

(a) n = 10   (b) n = 11   (c) n = 13

(d) n = 14   (e) n = 15   (f) n = 16

Figure 2: Sequence of snapshots of fractures propagating at each time step number n in 3D heterogeneous media. The blue regions corresponds to $\varphi < 0.1$. Both fractures grow non-planarly, then they join at $n = 11$ and start branching at $n = 13$.
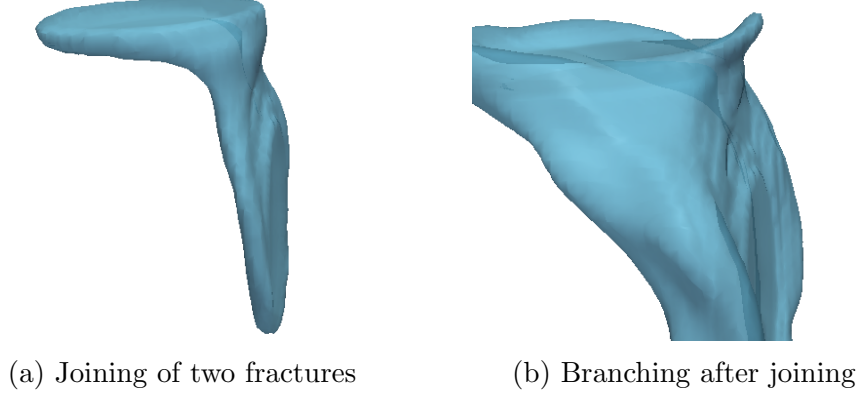
(a) Joining of two fractures   (b) Branching after joining

Figure 3: Detailed snapshots of the areas where the cracks are (a) joining at n=11 and (b) branching at n=13.
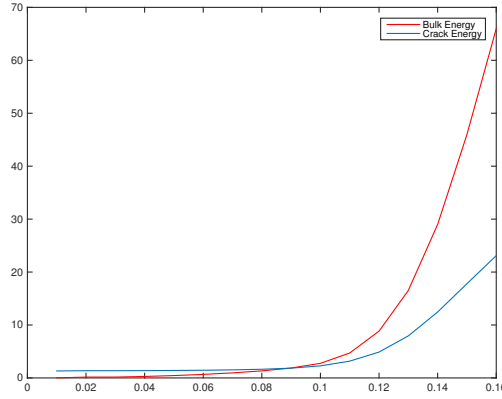

Figure 4: Evolution of bulk and crack energies. The crack energy starts increasing when the two fractures start growing at $n = 10$ (equal to $t = 0.1$). The bulk energy remains increasing even for propagating fractures since the applied pressure is still advanced.

5 CONCLUSIONS

In this work, we applied recently developed algorithms to compute three-dimensional pressurized-fracture propagation in heterogeneous media. The proposed method is efficient and robust. The novelty in comparison to existent literature is a detailed numerical simulation to show three-dimensional complex crack patterns, their forming, growth and joining.

REFERENCES

[1] Stefano Almi, Gianni Dal Maso, and Rodica Toader. Quasi-static crack growth in hydraulic fracture, 2014.

[2] M. Artina, M. Fornasier, S. Micheletti, and S. Perotto. Anisotropic mesh adaptation for crack detection in brittle materials. TUM Report, 2014.

[3] Wolfgang Bangerth, Timo Heister, Guido Kanschat, and Many others. *Differential Equations Analysis Library*, 2012.

[4] M. J. Borden, C. V. Verhoosel, M. A Scott, T. J. R. Hughes, and C. M. Landis. A phase-field description of dynamic brittle fracture. *Comput. Meth. Appl. Mech. Engrg.*, 217:77–95, 2012.

[5] B. Bourdin, C. Chukwudozie, and K. Yoshioka. A variational approach to the numerical simulation of hydraulic fracturing. SPE Journal, Conference Paper 159154-MS, 2012.

[6] B. Bourdin, G.A. Francfort, and J.-J. Marigo. Numerical experiments in revisited brittle fracture. *J. Mech. Phys. Solids*, 48(4):797–826, 2000.

[7] B. Bourdin, G.A. Francfort, and J.-J. Marigo. The variational approach to fracture. *J. Elasticity*, 91(1–3):1–148, 2008.

[8] S. Burke, Ch. Ortner, and E. Süli. An adaptive finite element approximation of a generalized Ambrosio-Tortorelli functional. *M3AS*, 23(9):1663–1697, 2013.

[9] G.A. Francfort and J.-J. Marigo. Revisiting brittle fracture as an energy minimization problem. *J. Mech. Phys. Solids*, 46(8):1319–1342, 1998.

[10] P. Gupta and C. A. Duarte. Simulation of non-planar three-dimensional hydraulic fracture propagation. *International Journal for Numerical and Analytical Methods in Geomechanics*, 38(13):1397–1430, 2014.

[11] T. Heister, M.F. Wheeler, and T. Wick. A primal-dual active set method and predictor-corrector mesh adaptivity for computing fracture propagation using a phase-field approach. ICES Report 14-27, Aug 2014.

[12] Michael Hintermüller, Kazufumi Ito, and Karl Kunisch. The primal-dual active set strategy as a semismooth newton method. *SIAM Journal on Optimization*, 13(3):865–888, 2002.

[13] Amit Katiyar, John T. Foster, Hisanao Ouchi, and Mukul M. Sharma. A peridynamic formulation of pressure driven convective fluid transport in porous media. *Journal of Computational Physics*, 261(0):209 – 229, 2014.

[14] C. Miehe, M. Hofacker, and F. Welschinger. A phase field model for rate-independent crack propagation: Robust algorithmic implementation based on operator splits. *Comput. Meth. Appl. Mech. Engrg.*, 199:2765–2778, 2010.

[15] C. Miehe, F. Welschinger, and M. Hofacker. Thermodynamically consistent phase-field models of fracture: variational principles and multi-field fe implementations. *International Journal of Numerical Methods in Engineering*, 83:1273–1311, 2010.

[16] A. Mikelić and M. F. Wheeler. Convergence of iterative coupling for coupled flow and geomechanics. *Comput Geosci*, 17(3):455–462, 2012.

[17] A. Mikelić, M.F. Wheeler, and T. Wick. A phase-field approach to the fluid filled fracture surrounded by a poroelastic medium. ICES Report 13-15, Jun 2013.

[18] A. Mikelić, M.F. Wheeler, and T. Wick. A quasi-static phase-field approach to the fluid filled fracture. ICES Report 13-22, submitted for publication, Aug 2013.

[19] A. Mikelić, M.F. Wheeler, and T. Wick. Phase-field modeling of pressurized fractures in a poroelastic medium. ICES-Preprint 14-18, Jul 2014.

[20] A. Mikelić, M.F. Wheeler, and T. Wick. A phase-field method for propagating fluid-filled fractures coupled to a surrounding porous medium. accepted for publication in SIAM Multiscale Modeling and Simulation, ICES Report 14-08, Jan 2015.

[21] A Settari and D A Walters. Advances in coupled geomechanical and reservoir modeling with applications to reservoir compaction. *SPE Journal*, 6(3):334–342, September 2001.

[22] T. Wick, G. Singh, and M.F. Wheeler. Pressurized fracture propagation using a phase-field approach coupled to a reservoir simulator. SPE 168597-MS, SPE Proc., 2013.

[23] T. Wick, G. Singh, and M.F. Wheeler. Fluid-filled fracture propagation using a phase-field approach and coupling to a reservoir simulator. ICES report 14-20, Aug 2014.